Computational aspects of the approximate analytic solutions of the SIR model: applications to modelling of COVID-19 outbreaks

COMPUTATIONAL ASPECTS OF THE APPROXIMATE ANALYTIC SOLUTIONS OF THE SIR MODEL. APPLICATIONS TO MODELLING OF COVID-19 OUTBREAKS

DIMITER PRODANOV[1,2]

[1] *Environment, Health and Safety, Leuven, IMEC, Leuven, Belgium*

[2] *ITSDP, IICT, Bulgarian Academy of Sciences, Sofia, Bulgaria*

Abstract. The SIR (Susceptible-Infected-Recovered) is one of the simplest models for epidemic outbreaks. The present paper derives the parametric solution of the model in terms of quadratures and derives a double exponential analytical asymptotic solution for the I-variable, which is valid on the entire real line. Moreover, the double exponential solution can be used successfully for parametric estimation either in stand-alone mode or as a preliminary step in the parametric estimation using numerical inversion of the parametric solution. A second, refined, asymptotic solution involving exponential gamma kernels was also demonstrated. The approach was applied to the ongoing coronavirus disease 2019 (COVID-19) pandemic in four European countries – Belgium, Italy, Sweden, France, Spain and Bulgaria.

Keywords: SIR model; Lambert W function; asymptotic analysis; incomplete gamma function; Gompertz distribution ORCID: 0000-0001-8694-0535

MSC: 92D30; 92C60; 65H05; 33-04; 33F05; 33B20

1. Introduction

Epidemic models have been steadily developed in the last 100 years. The coronavirus 2019 (COVID-19) pandemic, which became a global emergency in 2020, played the role of a catalyst for renewing the interest in epidemic models and resulted in a plethora of new developments. Interested readers are directed to the recent review of [1]. Since the pandemic is about ot enter its endemic phase new epidemiological tools, which can accurately predict the time course of different outbreaks, can be of considerable public utility for this and future outbreaks.

The SIR (Susceptible- Infected- Recovered) model was introduced by Kermack and McKendrick in 1927 under some simple assumptions, but it is still remains a very useful conceptual tool [2]. The SIR model is used to model epidemic outbreaks (see the monograph of Martcheva [3] or [4]). Outside epidemiology, SIR is also used in modeling of social networks, viral marketing, diffusion of ideas, spread of computer viruses, financial network contagion, etc. (see recent survey by Rodrigues and the references therein [5]). Very recently, some authors have convincingly demonstrated that the SIR epidemiological model can successfully model the short-term dynamics of COVID-19 outbreaks in 2020 for a number of countries [6, 7, 8, 9,

E-mail address: dimiter.prodanov@imec.be; dimiter.prodanov@iict.bas.bg.

10, 11]. Of course, the SIR model can be extended with an "Exposed" intermediate compartment, however such compartment is unobservable and most applied studies need to make additional assumptions to constrain the model parameters.

While sophisticated mathematical models may be desirable for simulating different control strategies, it is difficult to accurately estimate all necessary inputs. Therefore, relatively simple epidemiological models can turn out also to be of comparable merits.

Very early in the COVID-19 pandemic, it was also demonstrated by Carletti, Fanelli and F. Piazza that COVID-19 can be approximated by a SIRD model [12]. This was a very surprising finding given the sophistication of the present mathematical epidemiological literature. This result is supported by the findings in [13] where the deceased population could also be fitted by the SIR model.

The analytical solution of the SIR model was derived only relatively recently [14] as an equation of state between the phase space variables. As an alternative approach, Barlow and Weinstein derived a series for the S-variable and introduced rational convergents having better regions of convergence than the infinite series[10]. A different approximation scheme was introduced in [15]. Very recently, an inverse parametric solution for the I-variable has been also obtained [11, 13, 16].

The exact analytical solution of the SIR model can be computed by numerical inversion of a non-elementary integral equation for the I-variable by a Newton iteration (NI) scheme [13]. However, the numerical stability of the iteration scheme could not be thoroughly established in the original publication, since the asymptotic analysis of the model is non-trivial. The objective of the present work is to demonstrate an approximation scheme in terms of standard transcendental functions: exponents and gamma incomplete functions and to compare them with the previously introduced NI scheme. Moreover, the presented results rigorously demonstrate that the approximation scheme also provides asymptotic solutions for the incidence variable, which are valid on the entire real line. The purpose of the present work is not to argue about the advantages of SIR or another model but to demonstrate that asymptotic, closed-form models also have substantial merits.

2. Preliminaries of the SIR model

The SIR model is formulated in terms of 3 populations of individuals [3]. The S population consists of all individuals susceptible to the infection of concern. The I population comprises the infected individuals. These persons have the disease and can transmit it to the susceptible individuals. The R population comprises recovered individual who also cannot become infected and cannot transmit the disease to others. The dynamical formulation of the model comprises a set of three ordinary differential equations ODEs:

$$\dot{S}(t) = -\frac{\beta}{N} S(t) I(t) \tag{1}$$

$$\dot{I}(t) = \frac{\beta}{N} S(t) I(t) - \gamma I(t) \tag{2}$$

$$\dot{R}(t) = \gamma I(t) \tag{3}$$

By construction, the model assumes a constant overall population $N = S(t) + I(t) + R(t)$ [2]. The interpretation of the parameters is that a disease carrier infects on

average β individuals per day, for an average time of $1/\gamma$ days. The β parameter is called *disease transmission rate*, while γ – *recovery rate*. The average number of infections arising from an infected individual is then modeled by the number $R_0 = \beta/\gamma$, the *basic reproduction number*. Typical initial conditions are $S(0) = S_0, I(0) = I_0, R(0) = 0$ [2].

For simplicity of the presentation, the SIR model can be re-parametrized using time-rescaled variables as

$$\dot{s} = -si \tag{4}$$

$$\dot{i} = si - gi, \quad g = \frac{\gamma}{\beta} = \frac{1}{R_0} \tag{5}$$

$$\dot{r} = gi, \tag{6}$$

where $\tau = \beta t$.

Eq. 5 has a zero at $s = g$. Moreover, it is a maximum since

$$\ddot{i} = \dot{s}i + s\dot{i} - g\dot{i} = \dot{s}i = -si^2\big|_{i=i(\tau_m)} < 0$$

and all variables are positive defined.

3. Solution procedure

Since by construction, there is a first integral the system can be reduced to two differential equations in the phase planes (i, s) and (i, r), respectively:

$$\frac{di}{ds} = -1 + \frac{g}{s} \tag{7}$$

$$\frac{di}{dr} = \frac{s}{g} - 1 \tag{8}$$

In order to solve the model we will consider the two equations separately. Direct integration of equation 7 gives the first integral

$$i = -s + g \log s + c \tag{9}$$

where the constant c can be determined, for example, from the initial conditions.

3.1. **The s-variable.** The s variable can be determined by substitution in equation 4, resulting in the autonomous system

$$\dot{s} = -s\left(-s + g \log s + c\right) \tag{10}$$

which was solved implicitly by Harko [14]. The disadvantage of this formulation is that s is not an observable variable so it should be used only as an intermediate step to express the observable i or r variables.

3.2. **The i-variable.** The s variable can be represented explicitly in terms of the Lambert W function [17]. This allows for reduction of the original problem to an autonomous differential equation, which is implicitly solvable [13, 18]:

$$-\int \frac{di}{i\left(W_{\pm}\left(-\frac{e^{\frac{i-c}{g}}}{g}\right) + 1\right)} = g\tau \tag{11}$$

So the remaining task is to identify and interpret the integration constant.

3.3. **The r-variable.** The r variable can also be conveniently expressed in terms of i. For this purpose we solve the differential equation

$$\frac{dr}{di} = \frac{g}{s-g} = \frac{-1}{1 + W_{\pm}\left(-\frac{e^{\frac{i-c}{g}}}{g}\right)}$$

Therefore, $r = c_1 - g\log\left(-gW_{\pm}\left(-\frac{e^{\frac{i-c}{g}}}{g}\right)\right) = c_1 - g\log s$, following [13, 16]. Furthermore, $c_1 = g\log s^{\star}$ since $(s^{\star}, 0, 0)$ is a stable point. Therefore,

$$r = gW\left(-\frac{e^{\frac{i-c}{g}}}{g}\right) - i + c + c_1 \tag{12}$$

using the first integral. Since $(s^{\star}, 0, 0)$ is a stable point, it follows that the population size can be related to the integration constants as follows:

$$N = s^{\star} = c + c_1 = -gW_{-}\left(-\frac{e^{\frac{-c}{g}}}{g}\right) \tag{13}$$

where the first equality follows from the number conservation. Therefore, we can identify the integration constant

$$c = s^{\star} - g\log s^{\star} = N - g\log N \tag{14}$$

Finally,

$$r = gW_{\pm}\left(-\frac{e^{\frac{i-s^{\star}+g\log s^{\star}}{g}}}{g}\right) + s^{\star} - i \tag{15}$$

where the branch changes at a point determined by the parameterization used. The range of r is $\left[0, gW_{+}\left(-e^{-c/g}/g\right) - gW_{-}\left(-e^{-c/g}/g\right)\right]$ and the size of the epidemic outbreak is its supremum given by the quantity

$$r^{\star} = gW_{+}\left(-e^{-s^{\star}/g}\frac{s^{\star}}{g}\right) - gW_{-}\left(-e^{-s^{\star}/g}\frac{s^{\star}}{g}\right) \tag{16}$$

if there are no recovered individuals at the start of the outbreak.

4. The parametric solution

The parametric solution takes $t = 0$ as the position of the peak incidence i_m, although time shifting and formulation as initial value problem are straightforward to implement [16]. Remarkably, all involved integrals are non-elementary [13]. The parametric solution can be computed from eq. 9 and eq. 14:

$$\tau(s) = -\int_{g}^{s} \frac{dy}{y\left(g\log\left(y/s^{\star}\right) - y + s^{\star}\right)} \tag{17}$$

where the domain of s is $[-gW_{+}\left(-s^{\star}e^{-s^{\star}/g}/g\right), -gW_{-}\left(-s^{\star}e^{-s^{\star}/g}/g\right)]$.

The implicit solution eq. 11 can be computed as a definite integral, however this requires the computation of the Lambert W function on every integration step, which does not seem to be efficient. Alternatively, the solution can be computed more efficiently by substitution from eq. 17.

$$\tau(i) = -\int_{g}^{-gW_{\pm}\left(-\frac{s^{\star}}{g}e^{\frac{i-s^{\star}}{g}}\right)} \frac{dy}{y\left(g\log y/s^{\star} - y + s^{\star}\right)} \tag{18}$$

This equation involves computations of quadrature of only elementary functions, which are present in any numerical package.

Finally, to solve for $\tau(r)$ we differentiate eq. 12 by s to arrive at:

$$g\tau(r) = \int\limits_{g\log\frac{s^\star}{g}}^{r} \frac{e^{\frac{y}{g}}\,dy}{(y-s^\star)\,e^{\frac{y}{g}}+s^\star} \tag{19}$$

From the above we see that the population size $s^\star$ provides a natural foliation of the solution manifold.

4.1. **Peak value parameterization.** Alternatively, the solution can be parameterized by the global maximum of the i-variable i_m. This is especially beneficial for curve fitting since the raw data can fluctuate. In such case, $s_0 = g$ The link between the two foliations is provided by the equation $i_m = s^\star - g - g\log s^\star/g$ and consequently, the SIR model can be reformulated as

$$\tau(s) = -\int_g^s \frac{dy}{y\,(g\log y/g - y + g + i_m)} \tag{20}$$

$$\tau(i) = -\int_g^{-gW_\pm\left(-e^{\frac{i-i_m}{g}-1}\right)} \frac{dy}{y\,(g\log y/g - y + g + i_m)} \tag{21}$$

$$g\tau(r) = \int\limits_{s^\star-i_m-g}^{r} \frac{dy}{y - s^\star\left(1-e^{-\frac{y}{g}}\right)}, \quad s^\star = -gW_-\left(-e^{-\frac{i_m}{g}-1}\right) \tag{22}$$

As it turns out this form is especially suitable for parameter estimation from observed data.

Remark 1. *This author is grateful to the anonymous referee who brought into his attention the work of Kudryashov et al.* [18]. *In their recent work, these authors discussed the SIR and SIS models as epidemic tracking and warning tools. The authors obtained an equation, equivalent to eq. 22. In the present notation, the i variable is equivalent to the 2^{nd} order ODE*

$$i\ddot{i} + gi^3 + i^2\,\dot{i} - \dot{i}^2 = 0 \tag{23}$$

The starting equation of Kudryashov et al. is

$$nn_{tt} - n_t^2 + \alpha n^2 n_t + \alpha\beta n^3 = 0,$$

where the subscript denotes time differentiation. Dividing by β^2 and re-scaling time as in the rest of the present work $\tau = \beta t$ yields

$$nn_{\tau\tau} - n_\tau^2 + \frac{\alpha}{\beta}n^2 n_\tau + \frac{\alpha}{\beta}n^3 = 0$$

On the other hand, dividing by α^2 and re-scaling yields

$$nn_{\tau\tau} - n_\tau^2 + n^2 n_\tau + \frac{\beta}{\alpha}n^3 = 0$$

where now $\tau = \alpha t$. Therefore, we identify $g = \beta/\alpha$ for a match to be obtained.

The resulting eqs. 18a and b in the cited work correspond to the present eq. 22 by time and mass re-scaling. Unfortunately, the authors did not use it for fitting and parameter estimation purposes. Instead, they have used an approximation that

can be traced back to the original work of Kermack and McKendrick [2] *who develop asymptotics for* r *under the assumption that* r/g *is small. This corresponds to*

$$i_k(t) = i_m \mathrm{sech}^2\left(\sqrt{\frac{i_m}{2g}}\tau\right)$$

originally derived by Kermack and McKendrick [2] *and also stated in Kudryashov et al. The disadvantage of such an approach is that the hyperbolic secant approximation is symmetric, which does not correspond to the asymmetric shape of the i-variable (see Fig. 1). The curve's shape is approximated much better by the asymptotic equations to be presented in the next section.*

5. Approximation procedure

Since the SIR solution is non-singular anywhere in $\mathbb{R}$, one can make use of the Banach Fixed-Point Theorem. Notably, one can use the non-linear approximation scheme of Daftardar-Gejji-Jafari (DJM method) for solving the equivalent integral equations [19]. If we treat the equations of the SIR model as independent we can formally solve eq. 4 as

$$s(\tau) = s_0 e^{-\int i(\tau)d\tau}$$

On the other hand, eq. 5 can be transformed formally as

$$\dot{i} + gi = si \Longleftrightarrow e^{-g\tau} d\left(e^{g\tau} i\right) = si\, d\tau \Longleftrightarrow \frac{d\left(e^{g\tau} i\right)}{e^{g\tau} i} = s\, d\tau$$

Therefore, formally,

$$i(\tau) = k_2 e^{-g\tau + \int s(\tau)d\tau}$$

Starting from the 0^{th} order approximation $i^{(0)} \approx i_0$, it follows that $s^{(0)} \approx s_0 e^{-i_0\tau}$. However, this does not guarantee convergence of the iteration. To establish convergence we observe that $s = g$ is a fixed point of eq. 7 since $di/ds = 0$ for this point and, therefore, Banach theorem can be applied. Therefore, we must take $s_0 = g$ as an initial condition. This corresponds to the peak-value parameterization so that $i_0 = i_m$, $i'(0) = 0$ and

$$i(\tau) = i_m \exp\left(g \int_0^\tau e^{-\int_0^z i(y)dy}\, dz \, - g\tau\right) \tag{24}$$

can be formulated as a functional integral equation to be approximated by DJM. From the above integral equation the 1^{st} order approximation for the i-variable becomes the double exponential function

$$i^{(1)} = i_m\, e^{\frac{g}{i_m}\left(1 - e^{-i_m t}\right) - gt} \tag{25}$$

The second iteration of the DJM method results in a non-elementary Γ-integral as follows. Let

$$J := \int e^{\frac{g}{i_m}\left(1 - e^{-i_m \tau}\right) - g\tau} d\tau$$

Then, by change of variables $y = e^{-i_m\tau}$, the expression J can be recognized as a Γ-integral:

$$J = -\int y^{\frac{g}{i_m} - 1}\, e^{\frac{g}{i_m} - \frac{gy}{i_m}}\, dy\Big|_{y = e^{-i_m\tau}} = \frac{\Gamma\left(\frac{g}{i_m}, \frac{g}{i_m} e^{-i_m\tau}\right)}{\left(\frac{g}{i_m}\right)^{\frac{g}{i_m}}} e^{\frac{g}{i_m}}$$

where $\Gamma(a,x)$ is the upper incomplete Euler's gamma function. Therefore,

$$r^{(1)} = gJ = ge^{\frac{g}{i_m}} \frac{\Gamma\left(\frac{g}{i_m}, \frac{g}{i_m}e^{-i_m\tau}\right)}{\left(\frac{g}{i_m}\right)^{\frac{g}{i_m}}}$$

Then the second iteration step becomes

$$s^{(1)} = k_2 e^{-J} = k_2 \exp\left(-e^{\frac{g}{i_m}}\Gamma\left(\frac{g}{i_m}, \frac{g}{i_m}e^{-i_m\tau}\right)/\left(\frac{g}{i_m}\right)^{\frac{g}{i_m}}\right)$$

Matching the initial condition gives the value of the constant

$$k_2 = g\exp\left(\frac{-\Gamma\left(a,a\right)e^a}{a^a}\right), \quad a = \frac{g}{i_m}$$

Therefore,

$$s^{(1)} = g\exp\left(\left(\Gamma(a,a) - \Gamma\big(a, a\,e^{-i_m\tau}\big)\right)\left(\frac{e}{a}\right)^a\right), \quad q = \left(\frac{e}{a}\right)^a \tag{26}$$

Finally, following the same procedure for the i-variable we obtain

$$i^{(2)} = i_m \exp\left(g\int_0^\tau e^{q\left(\Gamma(a,a) - \Gamma\left(a, ae^{-i_m z}\right)\right)}dz - g\tau\right) \tag{27}$$

This is another non-elementary integral so if considered as a function of time, its values must be computed by quadratures. The asymptotics of the i-variable are compared with the parametric solution in Fig. 1.

The plot of the asymptotic solution for all variables is demonstrated in Fig. 2. The figure demonstrates the qualitative characteristics of the first-order approximated SIR model.

Remark 2. *Recently,* [20] *applied the Simple Equations Method (SEsM) to obtain approximate solutions of the SIR model. The correspondence with the present approach can be revealed as follows. From eq. 22 we formulate the autonomous system*

$$\dot{r} = gr - gs^\star\left(1 - e^{-r/g}\right)$$

Therefore,

$$\dot{r} = gr + gs^\star\sum_{k=1}^{\infty}\left(-\frac{1}{g}\right)^k\frac{1}{k!}r^k$$

The last equation is truncated to some finite number N, resulting in an approximate solution. For example, $N = 2$ results in the Bernoulli equation

$$\dot{r} = (g - s^\star)r + \frac{s^\star}{2g}r^2$$

which is exactly solvable. However, this approximation corresponds only to small values of r/g, which corresponds with the initial and final stages of an epidemic outbreak.

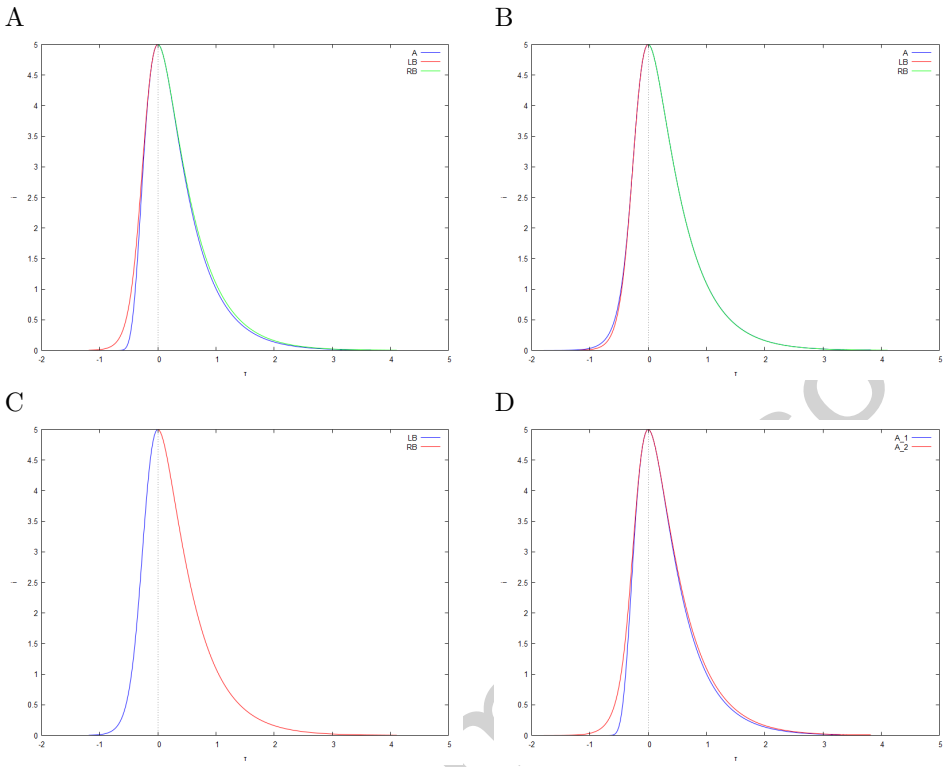

FIGURE 1. Comparison between parametric and asymptotic solutions $i(\tau)$

Asymptotic solutions compared to parametric plots of $(\tau(i), i)$ parameterized by $i_m = 5.0$ and $g = 2.0$. Legends: LB denotes the left branch involving $W_-(x)$, RB denotes the right branch involving $W_+(x)$, eq. 18. A denotes the asymptotic solution. A – the double exponential asymptotic for $i(\tau)$ is computed from eq. 25; B – the gamma-asymptotic for $i(\tau)$ is computed from eq. 27; C – the parametric solution $(\tau(i), i)$; D – comparison between 1st and 2nd order i-asymptotics. Plots were produced using the *quad_qags* Maxima numerical integration command.

6. The SIR model and some empirical distributions

In most interesting manner, the first asymptotic of the i-variable eq. 25 reveals a link to the empirical Gompertz density [21, 22]. This finding could be interpreted in the direction that in the cases where the Gompertz density "law" fits the data there could be an underlying multiplicative dynamics of the SIR type. The argument can be illustrated with the Gompertzian-SIR model of Borisov and Markov [23]. Briefly, the authors treat them SIR model as a chemical reaction network with an autocatalytic step, which is equivalent to the ODE system

$$\dot{s} = -\nu s$$
$$\dot{i} = ksi - \gamma i$$
$$\dot{r} = \gamma i$$

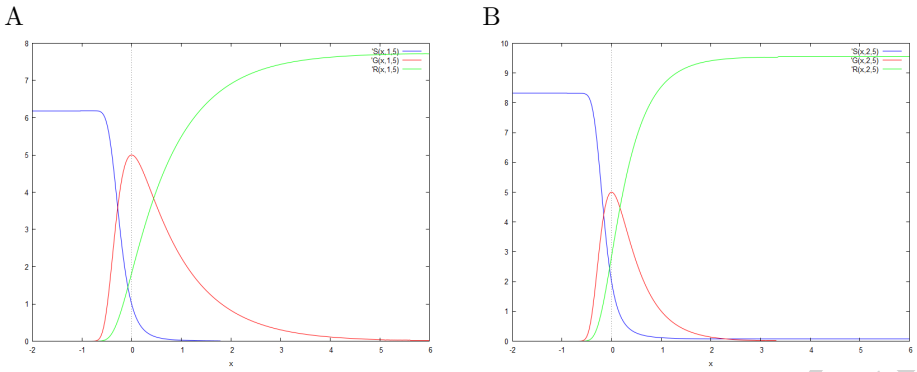

FIGURE 2. First order approximation of the SIR model
S, I, R denote the s(t), i(t) and r(t) first order approximations, respectively. A – g=1, $i_m = 5$; B – g=2, $i_m = 5$.

It is easy to see that the above system does not conserve the numbers, since

$$\dot{s} + \dot{i} + \dot{r} = (ki - \nu)s \neq 0$$

in general. The system is equivalent to the SIR model at the fixed point $i = i_m$ if $\nu = i_m k$, where the G-SIR model also conserves the numbers. Therefore, the G-SIR model, which is exactly solvable with solution $s(\tau) = s_0 e^{-\nu\tau}$,

$$i(\tau) = i_0 \exp(s_0 k/\nu(1 - e^{-\nu\tau}) - \gamma\tau)$$

(Prop. 16, [23]), is the asymptotic of SIR around the fixed point $i = i_m$. This is so because $s_0 = g$ at the fixed point and $k/\nu g = 1$ so that $k = 1$, $\nu = i_m$, $i_0 = i_m$ and $\gamma = g$ reproduces eq. 25 in our parameterization.

On the second place, the present asymptotic analysis reveals links to the Gumbel distribution [24, 25]. In his analysis of the SIR model Giubilei assumes empirically an exponential decay for $\beta(t)$. In contrast to the approach in [25], here the asymptotics are derived from first principles, that is the DJM algorithm [19].

7. Computational aspects

7.1. **Computation via the Wright Ω function.** There is another equivalent form of the system using another special function – the Wright Ω function [26] The $\Omega(x)$ function is defined as the solution of the equation

$$\log\Omega + \Omega = x$$

Using this formulation

$$W\left(-\frac{e^{\frac{i-c}{g}}}{g}\right) = \Omega\left(\frac{i-c}{g} - \log(-g)\right)$$

so that

$$\dot{i} = -ig\left(\Omega\left(\frac{i-i_m}{g} - 1 \pm j\pi\right) + 1\right)$$

where j denotes the imaginary unit to make distinction with the notation used for the SIR model. This is better suited for numerical evaluation at large arguments

as remarked by Corless and Jeffrey. The Ω formulation using Newtonian iteration was used for the MATLAB implementation of the solution.

The numerical schema is given briefly as follows. The principal branch starts from the initial approximation $w_0 = e^x$ while for the non-principal branch the iteration starts from $w_0 = -x - \log(-x)$.

$$dw_0 = x + w_0 - \log|x|$$
$$w_{n+1} = w_n + \frac{w_n(1 - dw_n)}{(1 - w_n)^2/w_n - dw_n/2w_n}$$

The iteration is continued until $\epsilon > \log|x| - w_n - x$, which is typically machine precision.

7.2. **Numerical approximation.** A Newtonian approximation schema can be derived for a given t as

$$i_0 = i_m\, e^{\frac{g}{i_m}\left(1 - e^{-i_m t}\right) - gt} \tag{28}$$
$$w_n = W_{\pm}\left(-e^{\frac{i_n - i_m}{g} - 1}\right) \tag{29}$$
$$i_{n+1} = i_n + g i_n\ (w_n + 1)\left(t - \int_g^{-g w_n} \frac{dy}{y\ (g \log y/g - y + i_m + g)}\right) \tag{30}$$

where we take the non-principal branch for $t < 0$ and the principal one for $t > 0$. This formulation has the advantage of requiring only one Lambert W function evaluation per step.

In a different implementation, instead of Lambert W function one can use the Ω function where

$$w_n = \Omega\left(\frac{i_n - i_m}{g} - 1 \pm j\pi\right) \tag{31}$$

On the other hand, the schema depends on numerical quadrature. The approximation schema is exact at $t = 0$ since then $i_0 = i_m$ and $w_n = W_{\pm}(-e^{-1}) = -1$. Therefore, $i_{n+1} = i_n$. The convergence of the method can be proven as follows. Let

$$|M_t| := \frac{1}{2}\left|\frac{i''(t)}{i'(t)}\right|$$

Then

$$|M_t| = \left|-\frac{e^{\frac{-i_m + i - g}{g} - W\left(-e^{\frac{-i_m + i - g}{g}}\right)}\left(-W\left(-e^{\frac{-i_m + i - g}{g}}\right) - 1\right)}{2\left(W\left(-e^{\frac{-i_m + i - g}{g}}\right) + 1\right)^2}\right|$$

where W denotes the appropriate branch of the Lambert W function. Using the appropriate identities of the function we obtain

$$|M_t| = \left|\frac{-W\left(-e^{-\frac{i_m}{g} + \frac{i}{g} - 1}\right)}{2\left(W\left(-e^{-\frac{i_m}{g} + \frac{i}{g} - 1}\right) + 1\right)}\right|$$

This quantity is bounded away from i_m in the i-variable. Indeed, suppose that $i < i_m$. Considering the range of the principal branch

$$-1 < W_+\left(-e^{-\frac{i_m}{g} + \frac{i}{g} - 1}\right) = A \leq 0$$

it follows that

$$M_t + \frac{1}{2} = \frac{-A}{2(A+1)} + \frac{1}{2} = \frac{1}{2(1+A)}$$

which is bounded if $A \neq -1$. For the non-principal branch

$$-\infty < W_- \left(-e^{-\frac{i_m}{g}+\frac{i}{g}-1}\right) = A < -1$$

holds. Then

$$M_t = \frac{-1}{2+\frac{2}{A}}$$

which is also bounded provided $A \neq -1$. Therefore, the schema has the desired quadratic convergence. From this analysis it can be noticed that the convergence of the method slows down as i approaches i_m. However, there to first order $i \approx i_0$.

Furthermore, define the logarithmic derivative as

$$q(t) := \frac{d \log i}{d \log i^{(1)}} = \frac{W_\pm \left(-e^{\frac{i-i_m}{g}-1}\right) + 1}{1 - e^{-i_m t}}$$

Therefore,

$$\frac{i(t)}{i_m} = \left(\frac{i^{(1)}(t)}{i_m}\right)^{q(t^*)}$$

by the mean value theorem. On the other hand, for $t > 0$

$$0 \leq W_+ \left(-e^{\frac{i-i_m}{g}-1}\right) + 1 \leq 1$$

since $W_+\left(-e^{-1}\right) = -1$ and $W_+(z)$ is monotone increasing in $z \in [-1/e, \infty]$. Therefore,

$$0 \leq q(t) \leq \frac{1}{1 - e^{-i_m t}}$$

On the other hand, around 0, by l'Hôpital's rule

$$\lim_{t\to 0} q(t) = \lim_{t\to 0, i\to i_m} \frac{-iW_\pm \left(-e^{\frac{i-i_m}{g}-1}\right) e^{i_m t}}{i_m} = 1$$

Also

$$q'(t) = \frac{e^{i_m t}\left(i(t) W\left(-e^{\frac{i(t)-i_m}{g}-1}\right) e^{i_m t} + (i_m - i(t))\, W\left(-e^{\frac{i(t)-i_m}{g}-1}\right) + i_m\right)}{\left(e^{i_m t} - 1\right)^2}$$

For $q'(t)$ after tedious calculations, involving l'Hôpital's rule, we obtain that $q'(0) = -i_m/2$, therefore 0 is a maximum. However, it is a maximum on the entire positive half axis as well by the above inequality. Therefore, $q(t) \in [0, 1]$ and

$$\frac{i(t)}{i^{(1)}(t)} = \left(\frac{i^{(1)}(t)}{i_m}\right)^{q(t^*)-1} \geq 1$$

Therefore, we can conclude that $i(t)$ dominates $i^{(1)}(t)$ as t grows from 0. On the other hand,

$$W_- \left(-e^{\frac{i-i_m}{g}-1}\right) + 1 \leq 0$$

and

$$q(t) = \frac{W_- \left(-e^{\frac{i-i_m}{g}-1}\right) + 1}{1 - e^{-i_m t}} \geq 0$$

since $W_-(z)$ decreases away from -1 for $z \in [-1/e, 0)$ while the sign of the denominator is negative. Since W is smooth at the branching point, we can employ the same calculations as above. Therefore, we can conclude that $i(t)$ dominates $i^{(1)}(t)$ as t decreases towards $-\infty$.

7.3. **Implementation.** All three integrals can be efficiently computed by numerical quadratures. Reference implementation on the Computer Algebra System Maxima has been developed and the code is available through the Zenodo repository [27]. Maxima incorporates an efficient numerical integration routine ported from QUADPACK [28]. The integration functions compute a result to a user specified accuracy. The numerical integrals were computed with relative precision 10^{-15}.

7.4. **Numerical experiments.** The Newton approximation is demonstrated in Fig. 4 using two parameter value combinations: $i_m = 6.0$ and $g = 1.0$, and $i_m = 7.0$ and $g = 1.5$, respectively. Computations have been preformed in MATLAB. The maximum number of iterations was set to 15 and the relative precision to 10^{-15} (Fig. 4 A,B) or 10^{-8} (Fig. 4 C,D). Slower convergence could be identified for the left solution branch. For the experiment with higher precision the approximation converged within 3 (g=1.0) to 4 (g=1.5) iterations in the majority of the time points. However, in some cases the maximal number of iterations was reached. For the lower precision experiment the right branch of *i(t)* consistently converged in 2 (g=1.0) or 3 steps (g=1.5). Slower convergence could be attributed to cancellation issues. Considering that the asymptotic solution already provides good approximation along the entire real line, absolute precision of 10^{-8} can be considered sufficient for most applications.

In a different experiment, using the same parameter values, a custom routine computing the Ω function was used. Results are demonstrated in Fig. 3.

The comparison of Figs. 3 and 4 demonstrates that the formulation using the Ω function has an advantage for lower absolute error setting.

8. Data sets

The COVID data sets were downloaded from the European Centre for Disease Prevention and Control (ECDC) website: `https://opendata.ecdc.europa.eu/covid19/casedistribution/csv`. The downloadable data file was updated daily until 14 Dec 2020 and contains the latest available public data on COVID-19 aggregated per country worldwide.

A second data set was downloaded on 15 Sept 2021. Inspection of the data set demonstrated that the new data started from 1 March 2021 and included the 31 countries from the European Economic Area (EEA). The data collection policy is available from `https://www.ecdc.europa.eu/en/covid-19/data-collection`.

9. Data Processing

The data were imported in the SQLite `https://www.sqlite.org` database, filtered by country and transferred to MATLAB for parametric fitting using native routines. Quadratures were estimated by the default MATLAB integration algorithms. Estimated parameter values were stored in the same database. The processing is described in [13], The parametric fitting was conducted using least-squares constrained optimization algorithm.

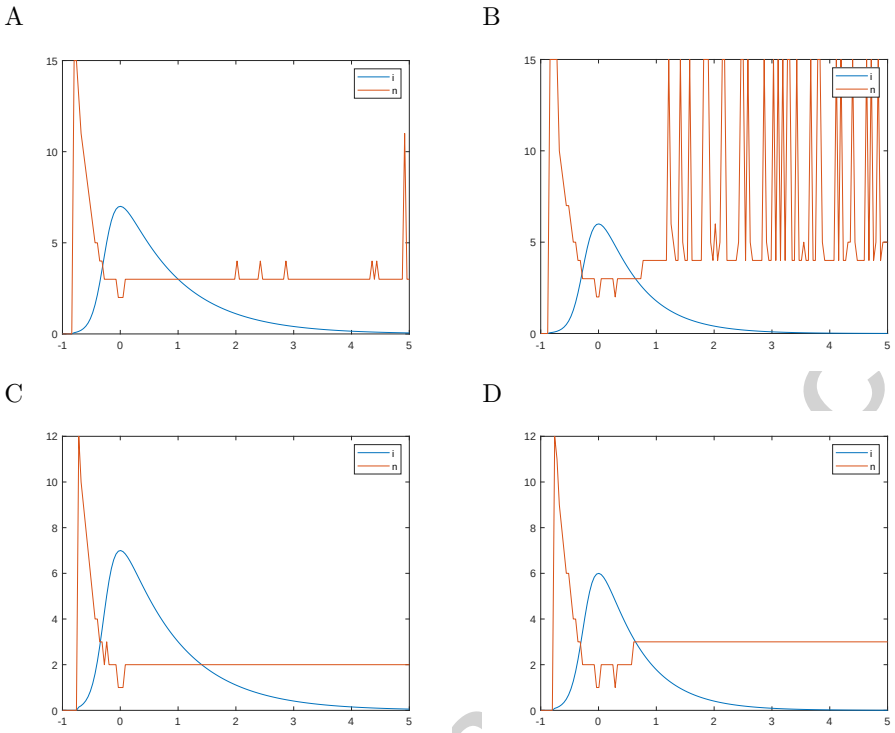

FIGURE 3. Numerical inversion of eq. 18
Legends: n – number of iterations; $i - i(t)$ A,C: $i_m = 7$ and $g = 1$; B,D: $i_m = 6$ and $g = 1.5$.

The least-squares constrained optimization was preformed using the fminsearchbnd routine [29]. The fitting model is given by

$$I_t \sim N \cdot i\,(t/10.0 - T|g, i_m)$$

where I_t is the observed incidence or case fatality, respectively. The model has 4 free parameters: N, T, g, i_m. For numerical stability reasons the time variable was rescaled by a factor of 10.

The goodness-of-fit (GOF) of the SIR model can be calculated in principle for all three variables. This, however, is not practical as only the I statistical variable is observed. Since R is by construction an increasing function, only the I statistical variable can be used for the purposes of the goodness-of-fit. Denoting the observed data vector by Y and the fitted model data by y, the goodness-of-fit measure can be defined as

$$R^2 := 1 - \frac{SS_{res}}{SS_{tot}}$$

where $SS_{tot} := \sum(Y - \bar{Y})^2$, $\bar{Y} := \sum Y/n$ and $SS_{res} := \sum(Y - y)^2$. In a similar way, the adjusted R^{2*} can be defined as

$$R^{2*} := 1 - \frac{SS_{res}/(n-k)}{SS_{tot}/(n-1)} \tag{32}$$

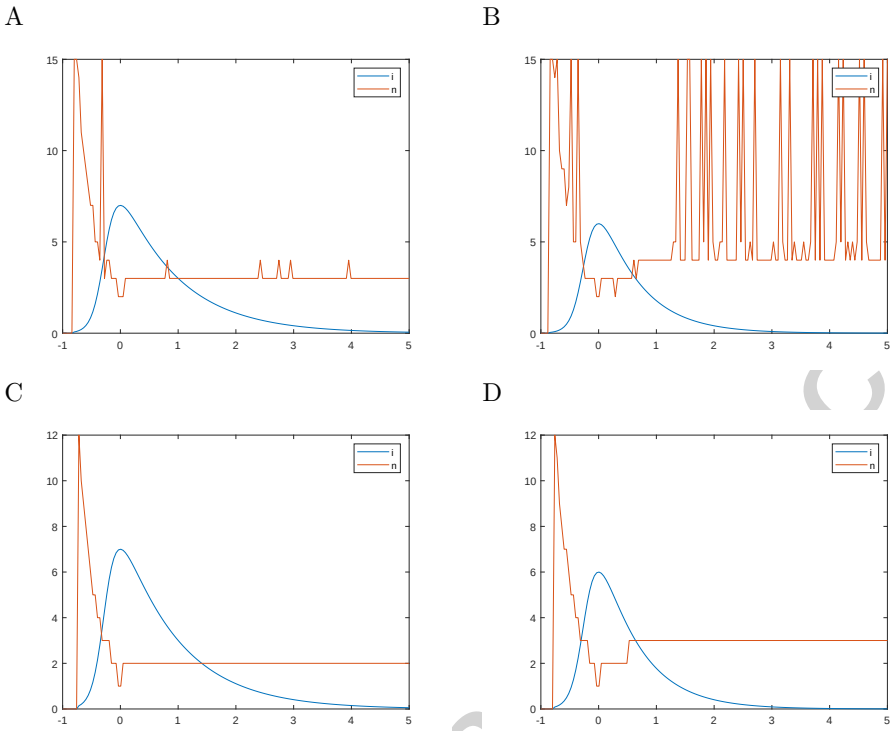

FIGURE 4. Numerical inversion of eqs. 18 using the Omega function iteration, eq. 31
Legends: n – number of iterations; i – $i(t)$ A,C: $i_m = 7$ and $g = 1$; B,D: $i_m = 6$ and $g = 1.5$.

where k is the number of free parameters and n denotes the length of the data vector.

10. Case Studies

10.1. **Analysis of the outbreaks in 2020.** The asymptotic approach is exemplified with data from ECDC for several European countries in the period Jan 2020 – Dec 2020. The data analysis in this section was limited to 14 Dec due to reporting reasons [13].

The goodness-of-fit for the SIR model was computed using eq. 32. The data for the case fatality and the incidence during the 1st COVID-19 wave are presented in Table 1.

The most direct and "brute-force" approach is to directly fit the time series using the numerical inversion scheme. Such an approach has been followed in the previous publication [13]. This incurs a relatively high computational cost associated with computation of integrals, followed by Newtonian iteration. Alternatively, the parameters can be fitted using the asymptotic eq. 25 only (see Fig. 5). Moreover, the asymptotic parameter estimation demonstrated faithful representation of the exact model (see Fig. 5). The numerical inversion approach is illustrated in Figs.

A B

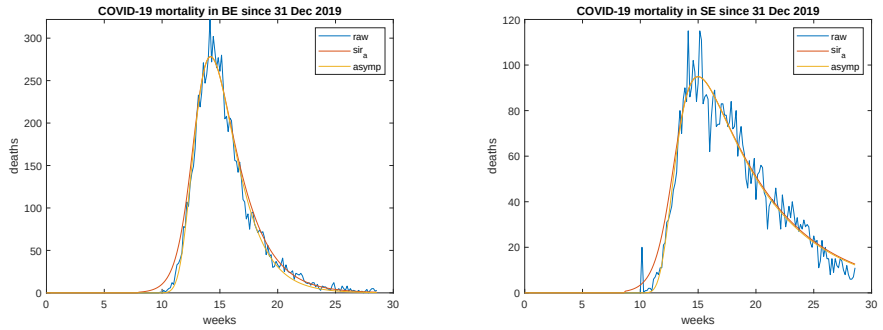

FIGURE 5. Case fatality parametric fitting for Belgium and Sweden Parametric fitting of the case fatality data of Belgium (A) and Sweden (B); 'asymp' refers to parametric fit using the asymptotic formula eq. 25, 'sir_a' refers to the i-variable computed by numerical inversion using the parameters estimated by eq. 25

data	R^{2*}	fitting type
	Belgium	
case fatality	0.999909	asymp
case fatality	0.999917	sir
incidence	0.9999387	asymp
incidence	0.999939	sir
	Sweden	
case fatality	0.9995981	asymp
case fatality	0.9996032	sir
	Italy	
case fatality	0.9999445	asymp
case fatality	0.9999459	sir
incidence	0.9999920	asymp
incidence	0.9999923	sir
	France	
case fatality	0.9998866	asymp
case fatality	0.9998885	sir
incidence	0.9999724	asymp
incidence	0.9999726	sir
	Spain	
case fatality	0.9998590	asymp
incidence	0.9999904	asymp

TABLE 1. GOF for the SIR model

'asymp' refers to fitting using asymptotic formula eq. 25 'sir' refers to fitting using numerical inversion of eq. 25. R^{2*} is computed according to eq. 32.

6 and 7, and compared to the asymptotic fitting in the subsequent tables. The raw

series for the incidence demonstrated pronounced weekly variation. However, this did not preclude successful parameter estimation.

The optimal fitting scheme involved three steps

(1) initial estimation from the raw data of the peak (i.e. incidence or case fatality data), the time to the observed peak and the initial guess $g_0 = 1$.
(2) asymptotic estimation of i_m, g, and T
(3) refined estimation of i_m, g, and T, involving numerical inversion of eq. 18.

Case fatality parameters for the first and second waves are presented in Tables 2 and 3. Incidence parameters are presented in Tables 4 and 5. From the data it is apparent that the new fitting procedure did not change parameter estimates for the countries with pronounced outbreaks. The estimates obtained using the method in [13] are marked with asterisks. In contrast, variation in the fitting could be observed for the first waves in Sweden and Spain. There the method did not converge well for the incidence and the data are not presented. This corresponded with the observed bimodal peak distributions in these countries.

Country	g	R_0	T[weeks]	i_m	fitting type
Belgium	0.7518	1.33	14.85	303.80	asymp
Belgium	0.7328	1.36	14.32	285.85	sir
Sweden	0.2082	4.80	15.80	89.05	asymp
Sweden	0.1952	5.12	15.68	90.48	sir
Italy	0.3942	2.54	12.74	764.05	asymp
Italy	0.3767	2.65	12.64	785.75	sir
France	0.6522	1.53	14.00	957.18	asymp
France	0.6186	1.62	13.93	989.53	sir
Spain	0.5807	1.72	13.18	851.03	asymp
Spain	0.5520	1.81	13.10	873.79	sir

TABLE 2. Case fatality parameters, first wave

T is given in weeks starting from 1st Jan 2020. 'asymp' refers to fitting using asymptotic formula eq. 25 'sir' refers to fitting using numerical inversion of eq. 25.

Country	g	R_0	T[weeks]	i_m	fitting type
Belgium	0.4913	2.06	44.8	201.88	sir*
Italy	0.3039	3.29	47.61	731.09	sir*
Belgium	0.5780	1.73	44.61	198.51	asymp
Belgium	0.5051	1.98	44.52	202.29	sir
Italy	1.5505	0.64	47.49	739.82	asymp
Italy	0.3479	2.87	47.34	734.07	sir
France	2.9215	0.34	45.93	589.25	asymp
Spain	0.5520	1.81	13.10	873.79	sir
Spain	0.5807	1.72	13.18	851.03	asymp

TABLE 3. Case fatality parameters, second wave

T is given in weeks starting from 1st Jan 2020. 'asymp' refers to fitting using asymptotic formula eq. 25 'sir' refers to fitting using numerical inversion of eq. 25.

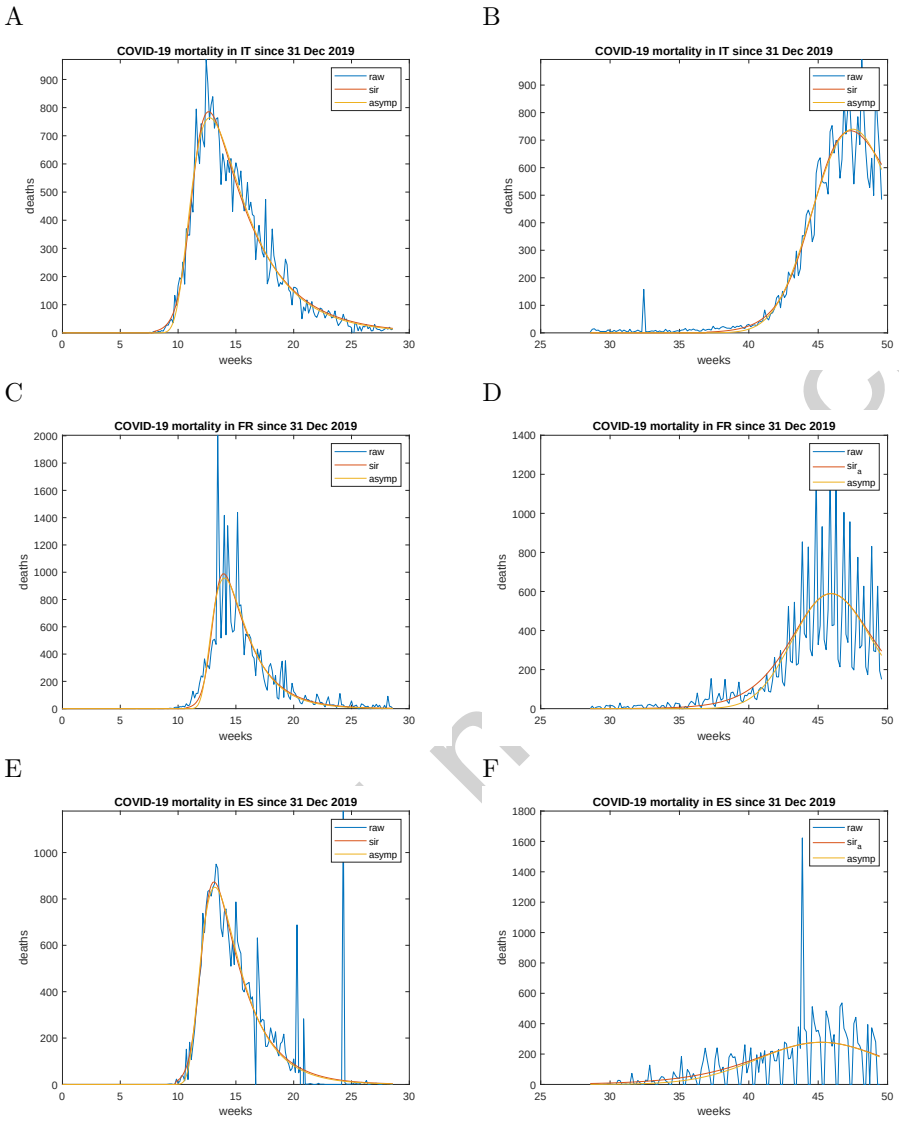

FIGURE 6. Parametric fitting of the case fatality data for the first and second waves in Italy, France, and Spain
A, B – case fatality fitting for Italy; C, D – case fatality fitting for France; E, F – case fatality fitting for Spain; 'asymp' refers to parametric fit using the asymptotic formula eq. 25, 'sir' refers to fitting the i-variable computed by numerical inversion starting from the parameters estimated by eq. 25. Note the pronounced weekly variation of the reported numbers.

The data demonstrate very good numerical (Tables 2, 3, 4, 5) and graphical agreement of both methods between themselves. Moreover, there is also an excellent agreement with the raw time series.

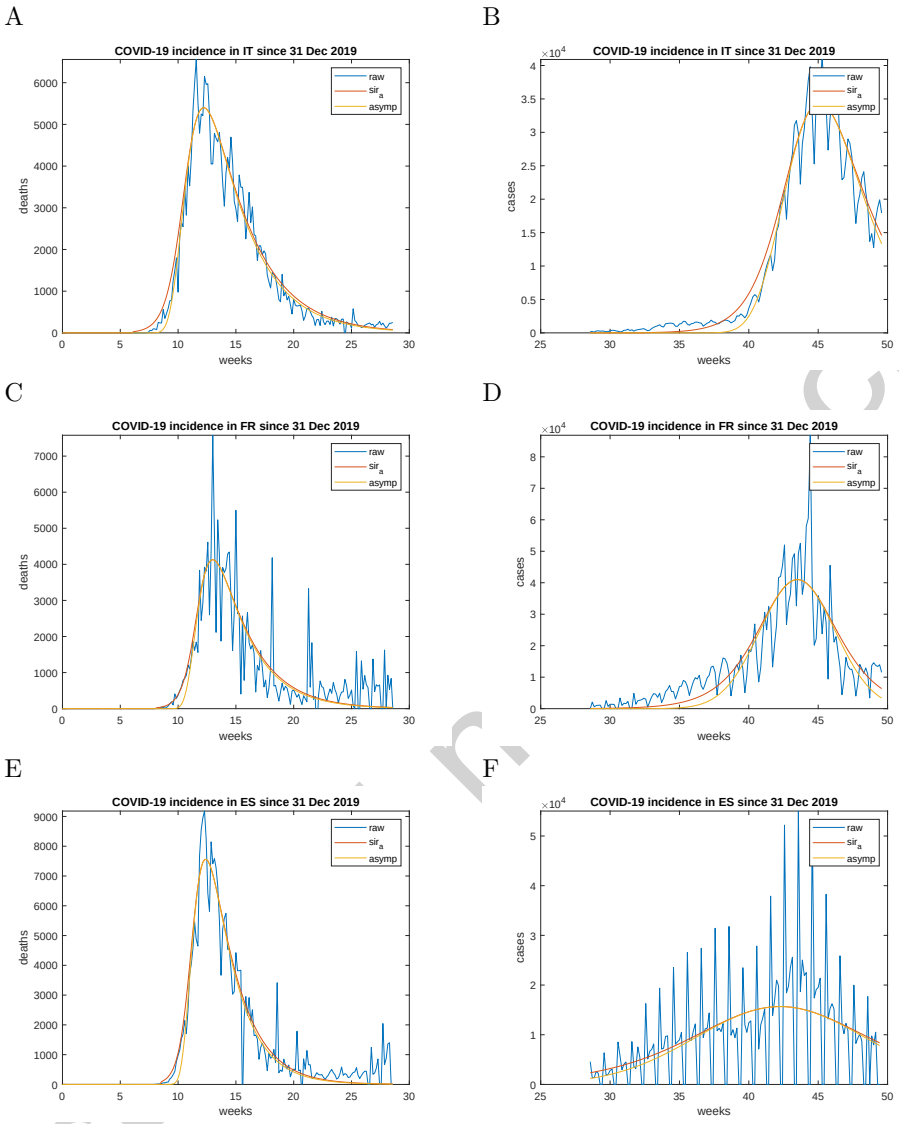

FIGURE 7. Parametric fitting of the incidence data for the first and second waves in Italy, France, and Spain
A, B – incidence fitting for Italy; C, D – incidencey fitting for France; E, F – incidence fitting for Spain; 'asymp' refers to parametric fit using the asymptotic formula eq. 25, 'sir_a' refers to computing the i-variable using the parameters estimated by eq. 25. Note the pronounced weekly variation of the reported numbers and the bimodal distribution of the data in France and Spain.

10.2. **Analysis of the outbreaks in 2021.** Bulgaria was selected for this case study since there was a recurring epidemic wave since Jul 2021 and the vaccination rate of the population remained low. The asymptotic approach is exemplified with

Country	g	R_0	T[weeks]	i_m	fitting type
Belgium	0.5500	1.82	14.00	1499.59	sir*
Italy	0.4006	2.50	12.30	5560.30	sir*
Belgium	0.5949	1.68	13.51	1495.37	asymp
Belgium	0.5991	1.67	13.51	1527.71	sir
Italy	0.4190	2.39	12.22	5401.13	asymp
Italy	0.3976	2.51	12.12	5557.86	sir
France	0.4899	2.04	13.00	4129.41	asymp
France	0.4808	2.08	12.97	4235.93	sir
Spain	0.6209	1.61	12.38	7565.90	asymp

TABLE 4. Incidence parameters, first wave

* – fitting method as used in [13]. T is given in weeks and refers to the time passed since 1st Jan 2020.

Country	g	R_0	T[weeks]	i_m	fitting type
Belgium	1.0000	1.00	42.43	14970.01	sir*
Italy	0.5548	1.80	45.25	34949.74	sir*
Belgium	1.3772	0.73	42.21	14642.57	asymp
Belgium	2.0921	0.48	42.29	15084.92	sir
Italy	0.7835	1.28	45.08	34412.50	asymp
Italy	0.5710	1.75	44.97	34963.18	sir

TABLE 5. Incidence parameters, second wave

* – fitting method as used in [13]. T is given in weeks and refers to the time passed since 1st Jan 2020.

data from ECDC for 2021, reported daily in the period 2 March – 15 Sept 2021. The data are summarized in Table 6. Plots are presented in Fig. 8.

g	R_0	T[weeks]	i_m	fitting type	wave
1.1307	0.88	36.18 (2020)	3465.44	sir*	second wave
0.7627	1.31	11.71 (2021)	3626.36	asymp	third wave
1.2007	0.83	11.81 (2021)	3663.88	sir	third wave
0.3254	3.07	35.28 (2021)	1483.91	asymp	fourth wave
0.1366	7.32	35.08 (2021)	1476.68	sir	fourth wave

TABLE 6. Incidence parameters, Bulgaria

* – fitting method as used in [13]. T is given in weeks and refers to the time passed since 1st Jan of the respective year.

From the results presented in Tables 3, 5, and 6 it is apparent that the asymptotic fitting of an ongoing outbreak can overestimate g (e.g. underestimate R_0) when the peak of the epidemic has not yet occurred. This effect can be observed also in Fig. 8.

11. Discussion

The present results can be discussed in three directions.

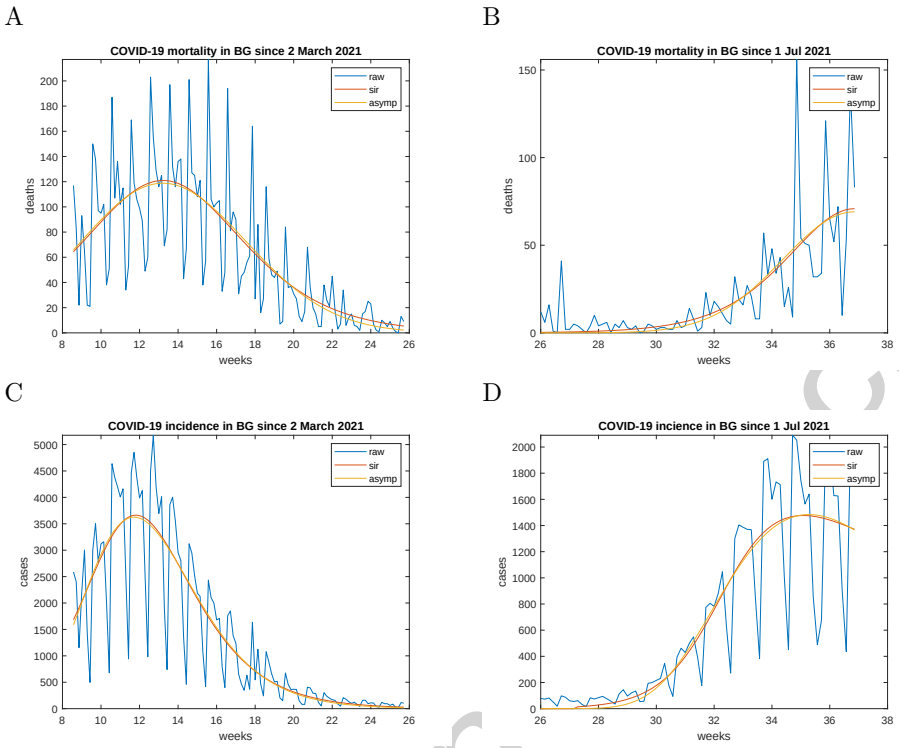

FIGURE 8. Third and fourth waves in Bulgaria
A,B – case fatality; C, D – incidence. Time is given in weeks and refers to the time passed since 1st Jan 2021. 'asymp' refers to parametric fit using the asymptotic formula eq. 25, 'sir' refers to fitting the i-variable computed by numerical inversion using the parameters estimated by eq. 25. Note the pronounced weekly variation of the reported numbers.

11.1. **Analytical implications.** The paper presents four solutions of the SIR model: two of them are approximate and asymptotic at the same time on the entire real line; one is the inverse parametric one, which has been identified before [14] and the fourth one uses the special function i(t) introduced in [13]. The 1st order solution i^1, which can be called Gompertzian, exhibits an interesting property. That is, the emergence of two fundamental time scales – a longer one determined by g and a shorter one determined by i_m. The presence of such a phenomenon is not apparent from the form of the differential equations only, as these explicate only the longer time scale g. Therefore, the appearance of the shorter scale is a truly emergent phenomenon.

The 2nd order solution i^2 (eq. 27), which can be called Gamma because of the appearance of the incomplete Γ function in the integral kernel, further increases the accuracy of the approximation to the analytical result. It retains the 2 scale property of the Gompertzian solution.

11.2. **Numerical implications.** The asymptotic analysis of the SIR model is important for the Newtonian approximation scheme since incorrect initial guess will

converge the iteration to the wrong branch of the Lambert W function. Therefore, one needs an initial function, which is dominated by the i-variable on the entire real line. The previous publication, which used Newtonian iteration [13], did not address the asymptotic analysis of the SIR model. Instead, the original asymptotic of Kermack and McKendrick and an ad hoc initialization function was used. However, this did not work for all combinations of parameters. The new asymptotic approach simplifies and stabilizes the data fitting procedure compared to [13]. The employed numerical procedures also demonstrate increased robustness to fluctuations demonstrated by the application to the COVID-19 data.

11.3. **Epidemiological implications.** A key finding of the presented results is that simple models are very useful in studying epidemic outbreaks also in the quantitative sense. This comes in contrast to some shared beliefs that models should be made more complicated to tackle real world epidemics [30]. Presented results demonstrate the utility of the SIR model for estimating the basic reproduction number and the peaks of the infections, respectively case fatalities in the COVID-19 pandemic outbreaks.

The paper introduces (pseudo-)adjusted R^2 criterion to measure the goodness of fit. It was demonstrated that both the Gompertzian and the analytic solutions provide en excellent fit to the data of the 1st COVID-19 wave in Belgium, Italy and France. In principle, one could introduce as well the asymptotic F-statistics for computation of a p-value, however the observed weekly periodicity of the data could make such an approach misleading.

There is a renewed interest in the applications of the SIR model in view of the COVID-19 pandemics [6, 7, 8, 9, 25, 31, 32]. Furthermore, Blanco et al. have performed fitting of the COVID-19 infections using the same data source, notably ECDC in the period Jan 2020 – Oct 2020 [33]. The authors have demonstrated the Gompertz model could fit very well ($R^{*2} = 0.998$) 25 out of the 28 countries in the data set amounting to 89% of the dataset. This corresponds with the data in Table 1. In similar way, the Gompertz function has been shown to be well fitted to the case fatalities for 73 countries compared by [34]. These findings correspond also with the findings of the present paper as per the discussion above relating the Gompertzian distribution and the SIR model.

12. Conclusion

In conclusion, the present paper demonstrates 2 approximate asymptotic solutions of the SIR model– one elementary and Gompertzian, and another one using numerical quadrature using an exponential Γ kernel. The exact solution is computed by numerical inversion of a non-elementary integral using numerical quadrature followed by Newtonian iteration. Starting from the elementary approximation, the convergence of the iteration is proven for the entire real line.

13. Funding

No specific funding available.

14. Conflicts of interest

The author declares no conflict of interest.

15. Availability of data and material

The COVID datasets were downloaded from ECDC using `https://opendata.ecdc.europa.eu/covid19/casedistribution/csv`. The analysis pertains to the version from 14 Dec 2020, which covers the period 1 Jan 2020 – 14 Dec 2021. A second dataset was downloaded on 15 Sept 2021. Inspection of the dataset demonstrated that the new data started from 1 March 2021 and covers the 31 countries from the European Economic Area (EEA).

16. Code availability

Reference implementation in the Computer Algebra System Maxima has been developed and the code is available through the Zenodo repository [27].

References

[1] S. K. Yadav, Y. Akhter, Statistical modeling for the prediction of infectious disease dissemination with special reference to COVID-19 spread, Frontiers in Public Health 9. doi:10.3389/fpubh.2021.645405.

[2] W. O. Kermack, A. G. McKendrick, A contribution to the mathematical theory of epidemics, Proceedings of the Royal Society of London. Series A, Containing Papers of a Mathematical and Physical Character 115 (772) (1927) 700–721. doi:10.1098/rspa.1927.0118.

[3] M. Martcheva, An Introduction to Mathematical Epidemiology, Springer US, 2015. doi:10.1007/978-1-4899-7612-3.

[4] H. W. Hethcote, The mathematics of infectious diseases, SIAM Review 42 (4) (2000) 599–653. doi:10.1137/s0036144500371907.

[5] H. S. Rodrigues, Application of SIR epidemiological model: new trends, International Journal of Applied Mathematics and Informatics 10 (2016) 92–97.

[6] S. Ahmetolan, A. H. Bilge, A. Demirci, A. Peker-Dobie, O. Ergonul, What can we estimate from fatality and infectious case data using the susceptible-infected-removed (SIR) model? a case study of covid-19 pandemic, Frontiers in Medicine 7. doi:10.3389/fmed.2020.556366.

[7] U. Nguemdjo, F. Meno, A. Dongfack, B. Ventelou, Simulating the progression of the COVID-19 disease in Cameroon using SIR models, PLOS One 15 (8) (2020) e0237832. doi:10.1371/journal.pone.0237832.

[8] E. B. Postnikov, Estimation of COVID-19 dynamics "on a back-of-envelope": Does the simplest SIR model provide quantitative parameters and predictions?, Chaos, Solitons & Fractals 135 (2020) 109841. doi:10.1016/j.chaos.2020.109841.

[9] N. R. Record, A. Pershing, A note on the effects of epidemic forecasts on epidemic dynamics, PeerJ 8 (2020) e9649. doi:10.7717/peerj.9649.

[10] N. S. Barlow, S. J. Weinstein, Accurate closed-form solution of the SIR epidemic model, Physica D: Nonlinear Phenomena 408 (2020) 132540. doi:10.1016/j.physd.2020.132540.

[11] N. A. Kudryashov, M. A. Chmykhov, M. Vigdorowitsch, Analytical features of the SIR model and their applications to COVID-19, Applied Mathematical Modelling 90 (2021) 466–473. doi:10.1016/j.apm.2020.08.057.

[12] T. Carletti, D. Fanelli, F. Piazza, COVID-19: The unreasonable effectiveness of simple models, Chaos, Solitons & Fractals: X 5 (2020) 100034. doi:10.1016/j.csfx.2020.100034.

[13] D. Prodanov, Analytical parameter estimation of the SIR epidemic model. applications to the COVID-19 pandemic., Entropy (Basel, Switzerland) 23. doi:10.3390/e23010059.

[14] T. Harko, F. S. N. Lobo, M. K. Mak, Exact analytical solutions of the susceptible-infected-recovered (SIR) epidemic model and of the SIR model with equal death and birth rates, Applied Mathematics and Computation 236 (2014) 184–194. doi:10.1016/j.amc.2014.03.030.

[15] M. Kröger, R. Schlickeiser, Analytical solution of the SIR-model for the temporal evolution of epidemics. Part A: time-independent reproduction factor., Journal of Physics A: Mathematical and Theoretical 53 (50) (2020) 505601. doi:10.1088/1751-8121/abc65d.
URL `https://doi.org/10.1088/1751-8121/abc65d`

[16] D. Prodanov, Comments on some analytical and numerical aspects of the SIR model, Applied Mathematical Modelling 95 (2021) 236–243. doi:10.1016/j.apm.2021.02.004.

[17] R. M. Corless, G. H. Gonnet, D. E. G. Hare, D. J. Jeffrey, D. E. Knuth, On the Lambert W function, Advances in Computational Mathematics 5 (1) (1996) 329–359. doi:10.1007/bf02124750.

[18] N. A. Kudryashov, M. Chmykhov, M. Vigdorowitsch, An estimative (warning) model for recognition of pandemic nature of virus infections, International Journal of Nonlinear Sciences and Numerical Simulation 0 (0). doi:10.1515/ijnsns-2020-0154.

[19] V. Daftardar-Gejji, H. Jafari, An iterative method for solving nonlinear functional equations, Journal of Mathematical Analysis and Applications 316 (2) (2006) 753–763. doi:10.1016/j.jmaa.2005.05.009.

[20] N. K. Vitanov, K. N. Vitanov, Epidemic waves and exact solutions of a sequence of nonlinear differential equations connected to the SIR model of epidemics, Entropy 25 (3) (2023) 438. doi:10.3390/e25030438.

[21] J. H. Pollard, E. J. Valkovics, The gompertz distribution and its application, Genus 48 (3/4) (1992) 15–28. doi:10.2307/29789100.
URL http://www.jstor.org/stable/29789100

[22] T. B. L. Kirkwood, Deciphering death: a commentary on gompertz (1825) 'on the nature of the function expressive of the law of human mortality, and on a new mode of determining the value of life contingencies', Philosophical Transactions of the Royal Society B: Biological Sciences 370 (1666) (2015) 20140379. doi:10.1098/rstb.2014.0379.

[23] M. Borisov, S. Markov, The two-step exponential decay reaction network: analysis of the solutions and relation to epidemiological SIR models with logistic and gompertz type infection contact patterns, Journal of Mathematical Chemistry 59 (5) (2021) 1283–1315. doi:10.1007/s10910-021-01240-8.

[24] E. Gumbel, Les valeurs extrm̂es des distributions statistiques, Annales de l'Institut Henri Poincaré 5 (2) (1935) 115 – 158.

[25] R. Giubilei, Closed form solution of the SIR model for the COVID-19 outbreak in italy-doi:10.1101/2020.06.06.20124313.

[26] R. M. Corless, D. J. Jeffrey, The wright ω function, in: Lecture Notes in Computer Science, Springer Berlin Heidelberg, 2002, pp. 76–89. doi:10.1007/3-540-45470-5_10.

[27] D. Prodanov, Numerics for the SIR model, Zenodo (2020). doi:10.5281/ZENODO.8036497.

[28] R. Piessens, E. Doncker-Kapenga, C. W. Überhuber, D. K. Kahaner, Quadpack, Springer Berlin Heidelberg, 1983. doi:10.1007/978-3-642-61786-7.

[29] D. Errico, Fminsearchbnd, https://www.mathworks.com/matlabcentral/fileexchange/8277-fminsearchbnd-fminsearchcon, mATLAB Central Exchange (2012).

[30] A. Huppert, G. Katriel, Mathematical modelling and prediction in infectious disease epidemiology, Clinical Microbiology and Infection 19 (11) (2013) 999–1005. doi:10.1111/1469-0691.12308.

[31] D. Fanelli, F. Piazza, Analysis and forecast of COVID-19 spreading in China, Italy and France, Chaos, Solitons & Fractals 134 (2020) 109761. doi:10.1016/j.chaos.2020.109761.

[32] I. Cooper, A. Mondal, C. G. Antonopoulos, A SIR model assumption for the spread of COVID-19 in different communities, Chaos, Solitons & Fractals 139 (2020) 110057. doi:10.1016/j.chaos.2020.110057.

[33] N. Blanco, K. A. Stafford, M. C. Lavoie, A. Brandenburg, M. W. Górna, M. Merski, A simple model for the total number of SARS-CoV-2 infections on a national level, Epidemiology and Infection 149. doi:10.1017/s0950268821000649.

[34] K. Rypdal, M. Rypdal, A parsimonious description and cross-country analysis of COVID-19 epidemic curves, International Journal of Environmental Research and Public Health 17 (18) (2020) 6487. doi:10.3390/ijerph17186487.